

Diffusion Gravity (10)
Evidence for MOND and Asymmetric Near-Field Gravity
from Asteroid 2000 BD19 Perihelia
DHFulton@ieee.org

Abstract

The close-approach of the Sun by asteroid 2000 B19 provides further evidence for MODified Newtonian Dynamics (MOND) and Asymmetric Near-Field (ASNF) gravity by observational data, which shows added acceleration along the elliptical orbit trajectory between the Sun's L1 point with the galaxy and the asteroid perihelion on November 5, 2021. This research posits that the object should increase in velocity due to MOND acceleration of $2.5 \times 10^{-11} \text{ m/sec}^2$ during the approach to perihelion, which can generate an additional velocity of $\sim 8 \text{ m/sec}$ that is measurable as a displacement along the elliptical orbit, resulting in an early passage through perihelion. Previous research already postulated that the anomalous acceleration of asteroid 1I/2017 U1 was clearly explainable by MOND acceleration in the solar flyby of that object, without exotic speculative scenarios. Herein is included an analysis of the ephemeris data of BD19 from NASA/JPL, which we then use to predict the MOND effect in the observational data.

Introduction

Evidence for MOND in *galaxies* abounds [14,29,30,31,34] through the work of McGaugh, Milgrom, Lelli, and others; so our goal in this report is to link observational evidence at the *solar system* level to MOND and a corresponding *physical mechanism-model*. The proposal herein is that the 2000 BD19 asteroid perihelion will provide further *direct* evidence for both MOND and ASNF - that galaxies generate *additional* control over their population of stars by the enormous “leverage” of galactic masses and distances, expressed through a *Galactic Scaling Ratio (GSR)* and the *Dirac Large Number Hypothesis (LNH)*, which together suggest a *near-field* radial acceleration for stars that orbit outside the MOND radius of the galaxy, $r_M = \sqrt{GM/a_0}$, where $a_0 = 1.2 \times 10^{-10} \text{ m/sec}^2$. This amplification model for the additional “leverage” of ASNF gravity may be the common element in MOND constant velocity rotation curves of galaxies. This report continues validation of the ASNF model with another direct solar system example in a specific asteroid passage very near the Sun, as a follow-up to our recent analysis for object 1I/2017 U1 Oumuamau [15]. The proposed model and trajectory of the asteroid 2000 BD19 (“BD19”) in its elliptical orbit of the Sun will show how MOND acceleration can be detected and measured within our solar system, but only when the object path is aligned to the galactic Lagrange point L1. The approach by the BD 19 object toward the L1 point to our host galaxy will take it directly through a “cone” of *asymmetric near-field (ASNF)* gravity, which will provide added acceleration, corresponding to the MOND acceleration, that is “required” to maintain the Sun at its constant orbital velocity of $\sim 230 \text{ km/sec}$. As a “test particle” the asteroid will be observed during a portion of its orbit by observers reporting to the Minor Planet Center [52] and used by NASA/JPL Horizons [36], which should confirm a slight increase in velocity that will result from MOND acceleration [], which will manifest by positional and time stamp data; which will be compared to the ephemeris *predicted* orbital model on the JPL Small Body Data Base. We propose this is as further supporting evidence for MOND within the solar system, which has been lacking [25,26], but now with this second “live” instance of a test particle approaching very near to the Sun, we will be confirming MOND acceleration near the Sun and its L1 point with the galaxy. The author introduced

ASymmetric Near Field Gravity (ASNF) in previous publications from April 2021 and October 2021 [15,16] as the underlying mechanism for MOND; this report adds another instance of asteroid acceleration to show not only that it corresponds to the MOND acceleration, but also that it localizes the effect into a conical volume of “near field” gravity in its close flyby perihelion of the Sun. Please refer to the summary and concept diagram *Figure 10-1*.

MOND acceleration is elusive to detect within our solar system; in many searches and Cavendish type experiments by Klein and others [25,27], the “scaling” requirement has been suggested as an important causal factor that precludes local detection. But size or scale, in and of itself, may not be the only determinant; in fact, we have shown in the previous work [15] that the MOND mathematical description by the interpolation function can be expressed as a geometric construct that relies on *galactic scale ratios* of mass and distance. The alignment with L1 (equipotential) of the galaxy and a near-field gravity that is amplified by the galactic scaling ratio combine to provide the needed MOND acceleration. Each star beyond the MOND radius of the galaxy will thereby be subject to this additional near-field amplified gravity, ensuring the acceleration required to minimize, through the *principle of least action*, the energy of the orbit by keeping it at constant velocity [Appendix 10-A-1]. We will demonstrate this additional near field gravity in the behavior of test particles, i.e., asteroids that align closely with and travel through the near-field cone and therefore undergo the same additional acceleration as does the Sun, *within* the L1 point to the galaxy. This report provides evidence for the effect upon BD19, as we did in the previous paper on 11/2017 U1.

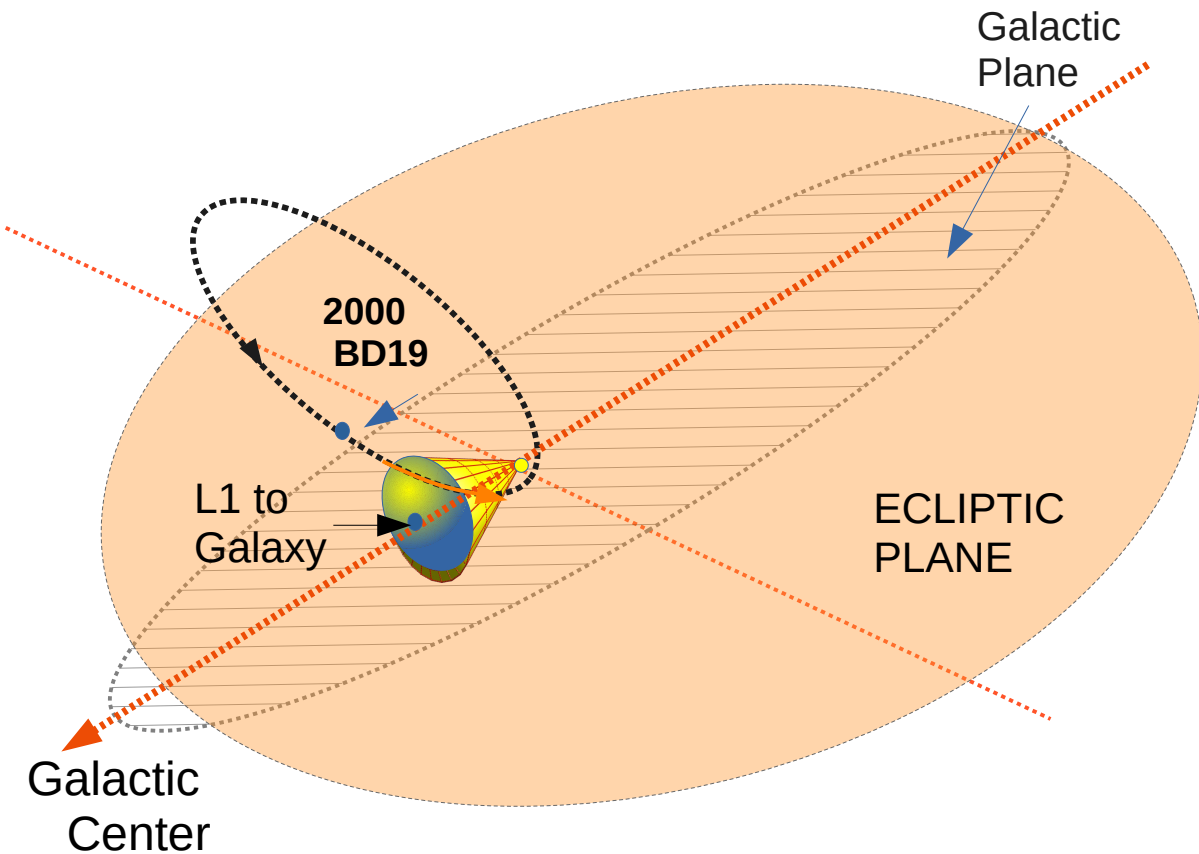


Figure : 10-1 Orbit of asteroid 2000 BD19 orientation to solar system and galaxy

We preface this analysis with a brief reference to other possible effects or alternative explanations that may have been proposed, or as factors known in the inner solar system planetoid orbits of similar objects.

Although other projects and publications by Micheli, Meech, Seligman [32, 33, 42, 49] have proposed explanations for the unusual or unexpected acceleration of asteroids, they typically lack sufficient data proof or clear cause-and-effect sequence, or magnitude [discussed by Katz, 24], i.e., they are too small, as in the case of the Yarkovsky effect, outgassing, or radiation pressure. Section 1b will elaborate some of the various alternative proposed explanations.

A diagram of the elliptical orbit of BD19 is provided in *Figure 10-2* which shows the orbit orientation

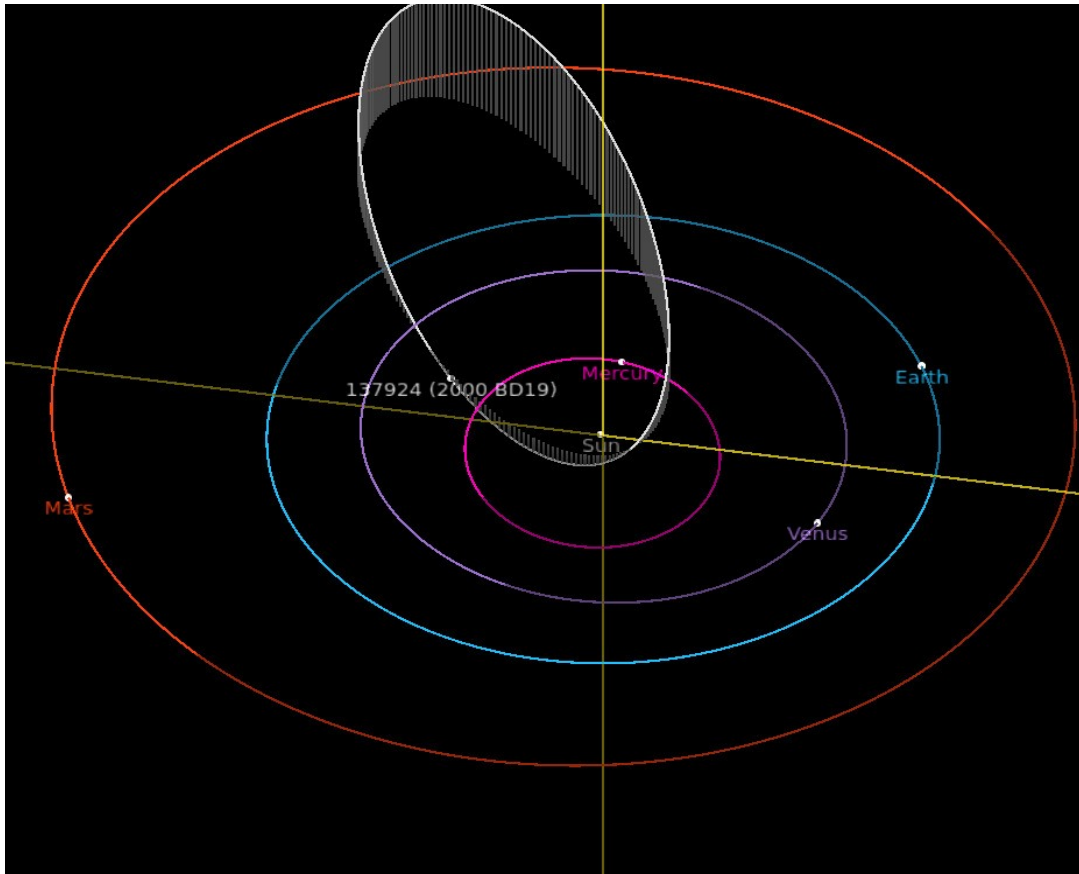


Figure 10-2 NASA/JPL Orbit Diagram of BD19 Relative to Inner Planets

to the ecliptic and the Sun, and inner planets. The orbit model is calculated and maintained by NASA/JPL Horizons [36] that is based upon over 780 data points (observations) used to update the ephemeris orbit model since discovery in January, 2000. The corresponding ephemeris data is summarized in Table 10-1, with important points of perihelion and the likely galactic L1 point calculated from our near-field gravity model. The most recent observation for BD19 was in April 2021. A major objective in this report is to use twenty perihelia data as a baseline to compare to expected current observation in December 2021 when the near-Sun flyby of BD19 is complete, which will then be incorporated as the most current clear evidence and confirmation of MOND acceleration in the near-field gravity influence from the galaxy.

We present the projected and predicted evidence – that will confirm MOND acceleration with the observed elliptical orbit data and calculations for the asteroid BD19 in Section 1. In Section 2, we show the direct linkage to MOND and the Diffusion Gravity model, and the passage through the *near-field* gravity cone as the causal mechanism for the excess, or “anomalous” acceleration of the asteroid. Sections 3 and 4 summarize the analysis and confirmation of the MOND-ASNF model and proposes further observational evidence in future occurrences of the alignment required with the host galaxy.

Section 1 The Orbit of 2000 BD19 and Acceleration due to MOND-ASNF

The asteroid perihelion passage provides a test particle and a test configuration to demonstrate both MOND and the causal DG model of asymmetric near-field gravity. This adds to the direct evidence already presented in the previous research [15], to support ASNF gravity models and their respective data and equations. Observers that provide data to the Minor Planet Center have not reported on the object or updated the “model” for the orbit of 2000 BD 19 since April 2021, mainly because it is not considered a threat to the earth. For the purpose of our analysis, however, we assume the data from NASA/JPL Small Body Data Base-Horizons [23] is accurate enough to perform calculations and to analyze the dynamics of the asteroid BD19. The important projected orbit position and time points for our analysis are summarized in Table 10-1, along with velocities as provided by the NASA/JPL ephemerides, to which we add the perihelion and our calculated L1 point distance from the Sun. We present again the calculations for MOND acceleration in the near field of our own Sun, and then use this resultant acceleration to project changes to the BD19 motion that can be expected due to the additional acceleration.

Starting from the fundamental MOND phenomenon, we know that it “provides” the shortfall of Newtonian acceleration in order to maintain a constant velocity for the Sun in its galactic orbit. In fact, we can simply derive the MOND “needed” acceleration for the Sun to maintain a constant velocity: The Newtonian acceleration of the Sun in its galactic orbit:

$$a_{NEWT} = \sqrt{(6.67430 \times 10^{-11} \text{ nt-kg})(9 \times 10^{10} \text{ solar mass})(1.9985 \times 10^{30} \text{ kg/sol-mass}) / (2.6 \times 10^{20} \text{ m})^2}$$

$$GM/r^2 = (12.01 \times 10^{30} / 6.76 \times 10^{40})$$

$$a_{NEWT} = 1.78 \times 10^{-10} \text{ m/sec}^2$$

where M is the estimated baryonic mass of the galaxy of 9×10^{10} solar mass, within the Sun’s radius, r_{SUN} to the galactic center as 2.6×10^{20} m. Similarly, the Mv^2/r Kepler law gives the *observed* centripetal acceleration

$$a_{ROT} = v^2 / r = (230 \times 10^3 \text{ m/sec})^2 / 2.6 \times 10^{20} \text{ m}$$

using $v_{Sun} = 230$ km/sec and r_{Sun} the distance of the Sun to the galactic center

$$a_{Rot} = 5.29 \times 10^{10} / 2.6 \times 10^{20} \text{ m/sec}^2$$

$$a_{ROT} = 2.03 \times 10^{-10} \text{ m/sec}^2$$

This straightforward calculation then allows us to calculate the “deficit” of acceleration from visible matter to the Keplerian *observed* centripetal acceleration as

$$a_{deficit} = a_r - a_{NEWT} = 2.03 \times 10^{-10} - 1.78 \times 10^{-10} \text{ m/sec}^2$$

$$a_{deficit} = 0.25 \text{ m/sec}^2 \times 10^{-10} \tag{1}$$

The “Simple” MOND interpolation function by Klein and by Zhao [25,50] can also be used to calculate the MOND acceleration as a very nearly an equal value to that obtained in equation (1). If this MOND acceleration, as derived from Newtonian mechanics, is applied to the asteroid in its

approach to the Sun through the “cone” of near-field gravity, as shown in *Figure 10-1*, for 134 hours (Table 10-1), i.e., from the estimated L1 point with the galaxy to the perihelion, the summed acceleration over that time period will result in an overall acceleration change of:

$$0.25 \text{ m/sec}^2 \times 10^{-10} (4.824 \times 10^5 \text{ sec}) = +12.06 \times 10^{-6} \text{ m/sec} \quad (2)$$

This MOND acceleration will induce a *velocity* increase that likely has the same cause as the “anomalous” acceleration for Oumaumau quoted in reference Micheli, et al. [32,33], of $4.92 \times 10^{-6} \pm 0.16 \text{ m/sec}^2$, with the difference being that with BD19, there is a longer time of travel through the cone of MOND influence. Both accelerations are consistent with the MOND acceleration, $2.5 \times 10^{-11} \text{ m/sec}^2$ exerted upon an object over the time and distance consistent with near-Sun gravity, and the orbital effects during perihelion. Also note that the orbit of BD19 is elliptical instead of hyperbolic, so the effect of the MOND acceleration should be observable in the orbit repeatedly, including the overall energy of the orbit and the distance of perihelion. In particular, we will compare the perihelion on November 5, 2021 with previous perihelia. A velocity gain should be measurable when observations can be made as the object emerges from the optical interference near the Sun. Unlike Oumaumau, however, this asteroid will be repeatedly detectable and trackable by monitoring instrumentation at observatories such as the ATLAS system [51], with long-term measurements that can support detection of MOND acceleration in the near-field of the Sun. Furthermore, the acceleration will apply to the object during its approach into the perihelion, which should therefore increase the velocity and affect the orbit accordingly. The increase *average* should be $\sim 6 \text{ m/sec}$, i.e., the application of acceleration

$$a_{\text{MOND}} = 2.5 \times 10^{-11} \text{ m/sec}^2$$

into the perihelion, including amplification by the near field:

$$\overline{\Delta v} = \frac{1}{2} \int_{L1}^{\text{Perih}} a_{\text{MOND}} \cdot dt = +6.03 \text{ m/sec} \quad (3)$$

where *L1* is the time of arrival into the MOND near-field, and *Perih* is the time of perihelion. This indicates a slightly “early” perihelion, in terms of the average velocity and the L1 distance travelled, of tens of seconds.

Table 10-1 Asteroid 2000 BD19 MOND Prediction Near Perihelion (NASA JPL SBDB [54])

Date	Time UTC	Ephemeris Position meters to Sun	Ephemeris Velocity km/sec	MOND adjusted Position= r_{Perih}	MOND adjusted Vel, m/s	Info-Comments Predictions
10/30/2021	00:00	4.609×10^{10}	-55.822	4.609×10^{10}	-55.822	NASA/JPL Ephemeris
10/31/2021	00:00	4.117×10^{10}	-58.239	4.117×10^{10}	-58.239	
10/31/2021	06:00	3.990×10^{10}	-58.861	3.990×10^{10}	-58.861	L1 to galaxy - Entry point
11/01/2021	06:00	3.471×10^{10}	-61.322	3.471×10^{10}	-61.522	$\Delta v = .2 \text{ m/sec}$
11/02/2021	06:00	2.932×10^{10}	-63.342	2.932×10^{10}	-64.052	$\Delta v = .75 \text{ m/sec}$ $\Delta r = 64.5 \text{ km}$
11/03/2021	06:00	2.381×10^{10}	-63.458	2.3819×10^{10}	-61.778	$\Delta v = 1.68 \text{ m/sec}$ $\Delta r = 218 \text{ km}$
11/04/2021	06:00	1.853×10^{10}	-56.809	1.8531×10^{10}	-53.819	$\Delta v = 2.99 \text{ m/sec}$ $\Delta r = 516 \text{ km}$
11/05/2021	20:00	1.457×10^{10}	-29.914	1.4571×10^{10}	-25.244	$\Delta v = 4.67 \text{ m/sec}$ $\Delta r = 1008 \text{ km}$
11/05/2021	20:20:38	1.3770384×10^{10}	.0121316	1.3773384×10^{10}	~ 0.0	PERIHEL $\Delta r_{\text{per}} = +3000 \text{ km}$

The BD19 orbit ephemeris is used to compare the actual MOND acceleration that is observed near the Sun. Observations and analyses confirm the MOND-ASNF added velocity in the data; the logical conclusion is that the cause is likely MOND near-field conical volume passage by an asteroid test particle. The historical perihelia analysis of the twenty orbits in this study shows the *mean* velocity increase has actually been $\Delta\bar{v} = +31.156 \text{ m/sec}$, as shown in Table 10-2; this positive Δv will likely persist into the future as a result of the increased acceleration by the MOND near-field. The increased velocity is a very small relative to the object's reference velocity of 135.1365961 km/sec, i.e., +0.00023. Nevertheless, this will manifest as increased orbital energy over time and number of orbits observed. The effect should be detectable as increased velocity and distance from the Sun. This amplified and localized near-field gravity supports and confirms the MOND paradigm at the solar system level.

Section 1b Other Influences and Elements Possible for BD19

This analysis has considered other effects that could be alternative explanations for near-field gravity effects close to the Sun; these are listed below and each are discussed.

1. Modeling “osculating elements” (when selected) in the Horizons JPL Small Body Data Base. The SBDB allows researchers to incorporate effects from the various inner solar system n-body perturbations, as well as the general relativistic effects from the Sun. We assume in our analysis that the model includes minor known perturbations; and the effects are reflected in the ephemeris, therefore we do not manually adjust the data or otherwise compensate. The primary important consideration is the number and quality of observations incorporated into the orbital models, which allows for the important trends to be discerned, apart from the JPL-adjustments. Our analysis objective is to show these trends and the implied acceleration that can cause the increase in velocity as well as distance at perihelion of the object.

2. Other planetary bodies. The effect of inner solar system planetoids has been modeled by various researchers and simulations, so the major effects, or resonances are characterized [43,21]. Asteroids have been studied in numerous simulations and n-body dynamical analyses and data. Examples that include BD19 are covered in [28]. Our analysis assumes that the major effects of inner planetoids are included as the observations are used to update the Horizons data base, and that the effect of Venus and Mercury have been extensively studied and incorporated. There is no doubt as to the resonances and inner planet influences, which result in osculations and periodic or cyclical orbital effects. Our analysis here is specific to longer term cumulative orbit changes due to the galactic MOND acceleration, which should be discernible from other periodic effects.

3. External Field Effects (Milgrom et al.). These have been studied as possible MOND influences at the solar system level; however, the DG theory of ASNF exists only in the near-field of the Sun, and specifically in alignment with the Galactic L1 point, which is unlike the more ubiquitous EFE proposed by Blanchet and Novak [7], and Milgrom [35] as well as others.

4. Minor effects: This includes Yarkovsky, radiation pressure, outgassing. These various effects have been studied and are generally small compared to the MOND acceleration presented herein. The Yarkovsky effect ($<10^{-12}$) [43] is size-dependent; for kilometer-sized asteroids, the Yarkovsky effect is minuscule over short periods: the force on a half-kilometer asteroid has been estimated at a net acceleration of 10^{-12} m/s^2 [49] for example, on asteroid 6489 Golevka. Likewise, radiation pressure may also be operative, but only for large and thin surface areas (BD 19 is less ~ 1 km in diameter). The fact that the asteroid approaches very near the Sun results in its heating on the Sun facing side;

however the BD19 object is *rotating* at the rate of 10.57 hours, so any heating or other effect of intense radiation would be uniform as the object travels through perihelion.

The analysis herein is to show the longer term, and substantial near-field MOND effect relative to minor effects, that will appear as increases in the orbital velocity and distance, and therefore orbital energy of the asteroid, and not just as cyclical perturbations. . We assume for our study, then, that minor effects do not generate a comparable magnitude Non-Gravity Acceleration (NGA) propulsion, relative to the MOND near-field and the Sun’s gravity itself.

5. Precession of Perihelion. Measurement of general relativistic *beta* and *gamma* has been proposed by Margot [28] as an area of investigation for the general relativistic precession on BD19, which is projected to have ~26 arc seconds of precession per century. General relativity requires highly accurate measurement capability of radar and astrometry, implying a very small magnitude effect. Margot’s proposal assumed availability of the Arecibo observatory for accurate tracking, but that was prevented by extensive damage to that observatory. The precession of BD19 is small, but should be detectable in the observational data year-to-year, with 0.26 arc seconds of precession per orbit. This is smaller than the amount of offset in distance from our analysis of 3000 km, or .053, which is to say that this is not a substantial factor relative to our MOND acceleration. This translates to approximately 160 km, or $\sim 1.6 \times 10^5$ m. advance to the perihelion per year. The author previously analyzed and reported [17] the precession of Mercury as a galactic gravity effect; likewise this can be applied in this case, where the precession of BD19 is also attributed either directly or indirectly, i.e., by MOND or galactic gravity. The previous work by the author proposed galactic gravity as an alternative cause of “extra” precession of Mercury, rather than general relativity. In this current study, we maintain that approach, i.e., that the effect of galactic gravity, i.e., MOND, is large enough in the near-field conical volume, to explain both general relativity as well as the direct MOND near-field gravity that causes the increasing velocity and distance of object BD 19 over a course of twenty orbits.

The above considerations include periodic resonance effects of the inner planets; simulations and numerical analyses, which seem to comprise the bulk of the research and studies of the motions of the inner solar system planetoids, and that observations are at best only periodic, due to the fact that this object is not a threat to earth and is therefore not covered under the Near Earth Object monitoring programs, except incidentally. Nevertheless, the Horizons program is important for NEO studies, and yields useful results for BD19, as relate to our MOND and near-field gravity analyses.

This report’s objective is to identify the Asymmetric Near Field (ASNF) gravity and MOND as the probable source of additional acceleration of BD19 during its perihelion approach.

Section 1c Analysis of Data From Previous Perihelia

A dynamical analysis of the data from observations and the JPL Horizons ephemeris shows an increase in the orbit *velocity near perihelion*, according to the *vis viva* equation and orbital calculations:

$$v^2 = GM \left(\frac{2}{r} - \frac{1}{a} \right) \tag{4}$$

where *G* is the gravitational constant *G*, *M* is the mass of the Sun, *r* is *r_p* the distance at perihelion, and *a* the semi-major axis of the elliptical orbit. This equation is used to obtain the velocity at perihelion for each orbit considered from 2005 to 2021 (twenty orbits). The velocity at each perihelion was then

compared to the baseline computed velocity obtained from reference JPL data for the velocity at perihelion, using their provided values:

$$\begin{aligned}
 V_p &= 135.1365961 \times 10^5 \text{ m/sec} && \text{velocity at perihelion (from equation 4)} \\
 a_{BD19} &= 3.1118194 \times 10^{11} \text{ m} && \text{semi-major axis of elliptical orbit (JPL)} \\
 GM &= 1.32718456 \times 10^{20} \text{ m}^2/\text{sec}^2 && \mu = GM = \text{gravitational constant} \cdot \text{mass of Sun} \\
 r_p &= 1.3771058377 \text{ m} && \text{JPL reference distance perihelion}
 \end{aligned}$$

Thus we can calculate, using JPL Horizons data, a “reference” velocity of 135.1365961 km/sec or 135136.5961 m/sec, and as presented in Table 10-2, a mean velocity of 135.1677523 m/sec, and an increase of $\overline{\Delta v_p} = +31.1565$ m/sec over twenty orbits.

Table 10-2: Compared Elements of Orbit Model due to MOND Acceleration and ASNF

Year	Date - UTC	Velocity _{perihel} v _{ref} =135.1365961	Δv_p m/sec $\Delta v_\mu = + 31.16$	Distance r_p $\times 10^7$ km	$\Delta r_p =$ km	$\xi =$ J/kg $\times 10^8$
2005	06-08 13:11	135.1791340	+ 042.5379	1.376284765	-06928.90	-5.0610469
2006	04-04 05:51	135.1713114	+ 034.7253	1.376435821	+00541.83	-5.0610469
2007a	01-28 23:19	135.1852672	+ 048.6711	1.376166441	-08112.14	-5.0610470
2007b	11-24 05:51	135.2035870	+ 066.9909	1.375813096	-11645.59	-5.0610470
2008	09-19 09:59	135.2084541	+ 071.8580	1.375722849	-12548.06	-5.0610469
2009	07-16 03:26	135.2012835	+ 064.6874	1.375857518	-11201.37	-5.0610470
2010	05-11 20:36	135.1751780	+ 038.5819	1.376361093	-06165.60	-5.0610470
2011	03-07 13:51	135.1480974	+ 011.5013	1.376883767	-00938.70	-5.0610470
2012a	01-01 06:56	135.1351001	- 001.4960	1.377134572	+01569.18	-5.0610470
2012b	10-26 23:46	135.1543936	+ 017.7975	1.376762220	+02154.30	-5.0610469
2013	08-22 16:37	135.1910462	+ 054.4501	1.376054962	-09226.93	-5.0610469
2014	06-18 09:56	135.2061625	+ 069.5664	1.375763432	-12142.34	-5.0610470
2015	04-14 03:09	135.1759910	+ 039.3950	1.376345407	-06322.47	-5.0610470
2016a	02-07 20:27	135.1338567	- 002.7394	1.377158739	+01810.85	-5.0610469
2016b	12-03 13:49	135.1109649	- 025.6312	1.377600923	+06232.69	-5.0610469
2017	09-29 06:50	135.1940759	+ 057.4798	1.377224973	+02473.29	-5.0610469
2018	07-25 23:42	135.1251725	- 011.4326	1.377326459	+03488.05	-5.0610470
2019	05-21 16:55	135.1415182	+ 004.9221	1.377010793	+00331.39	-5.0610470
2020	03-16 10:12	135.1585678	+ 021.9717	1.376681646	-02960.08	-5.0610470
2021a	01-10 03:11	135.1558837	+ 019.2876	1.376446956	-02342.00	-5.0610470
2021b	11-05 20:20	pending obs	pending	pending	pending	pending
2021b	Prediction by ASNF grav	135.2061000 km/sec	$\overline{\Delta v} = +8.04$ m/sec	$+3.0 \times 10^6$ m 1.377250000	$\overline{\Delta r_p} = -3546.63$	-5.0610470 $\times 10^8$ J/kg

Assuming the JPL database is accurate, the mean of velocity deviations over twenty orbits shows an increase over the expected velocity, as shown in Table 10-3. In a predictive sense, then, a velocity

increase should be expected in the ephemeris data. That would provide evidence of an “anomalous” effect of either nearby planetoids, or the MOND effect itself, or a combination of both. Our emphasis here is to show the MOND effect between the Sun and the L1 point with the galaxy, i.e., there is an amplified gravity in that conical volume near the Sun. BD19 can provide the empirical evidence of that gravity by its behavior in velocity (acceleration) and distance at perihelia. Using a similar approach we also analyze the variation in distance at perihelion, also presented in Table 10-2, to show a mean distance r_p at perihelion, with Δr_p of -3546.63 km., but with a definite up-trend, which is shown in *Figure 10-3*. The reference distance r_{REF} shown is that of the JPL quoted perihelion distance. *Figure 10-3* provides only the scaling and slope for difference values over a 1.37500×10^{10} meter baseline, which shows the up-trend in r_p distance, and thus a rise in the perihelion distance of BD19. This we present as further evidence for causality from MOND acceleration in near-field gravity zone. The linear regression of the data was computed with a readily available tool [20] to demonstrate the obvious trend upward for the twenty orbits studied.

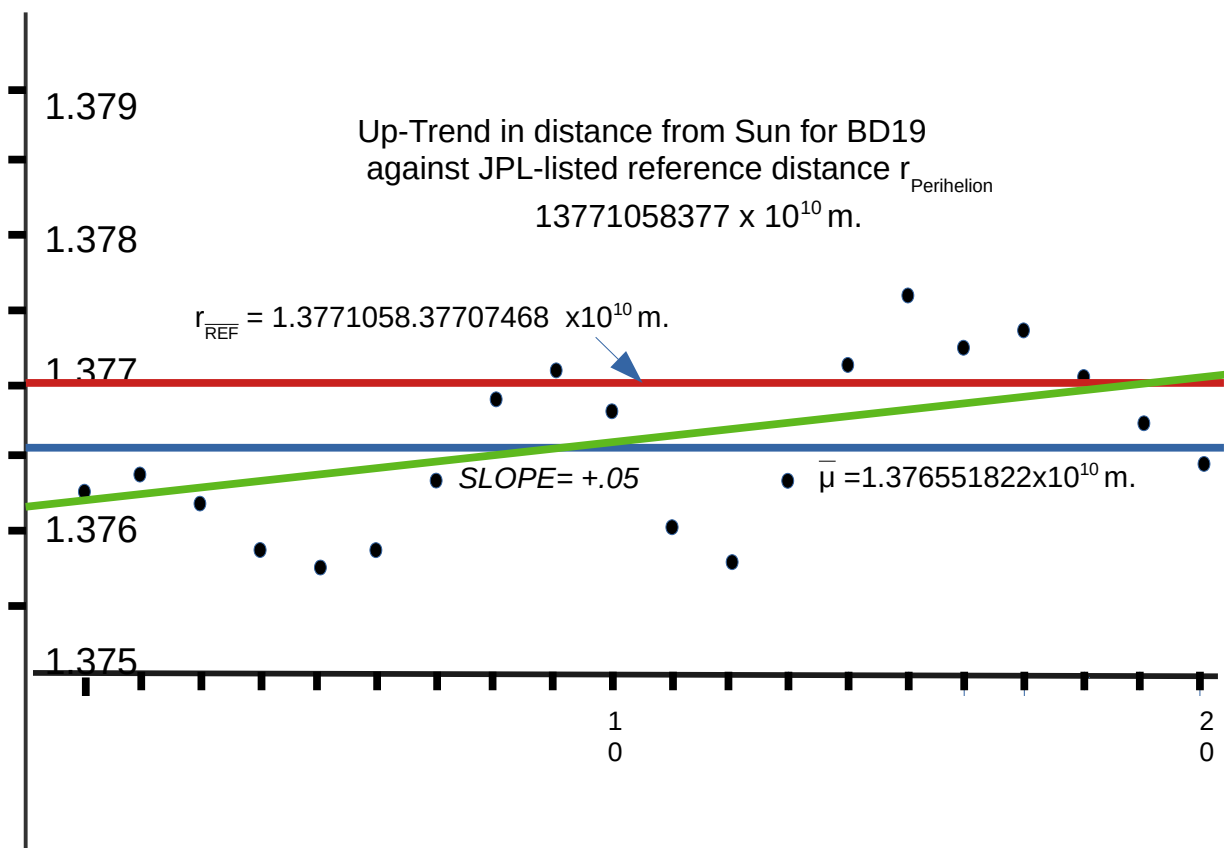
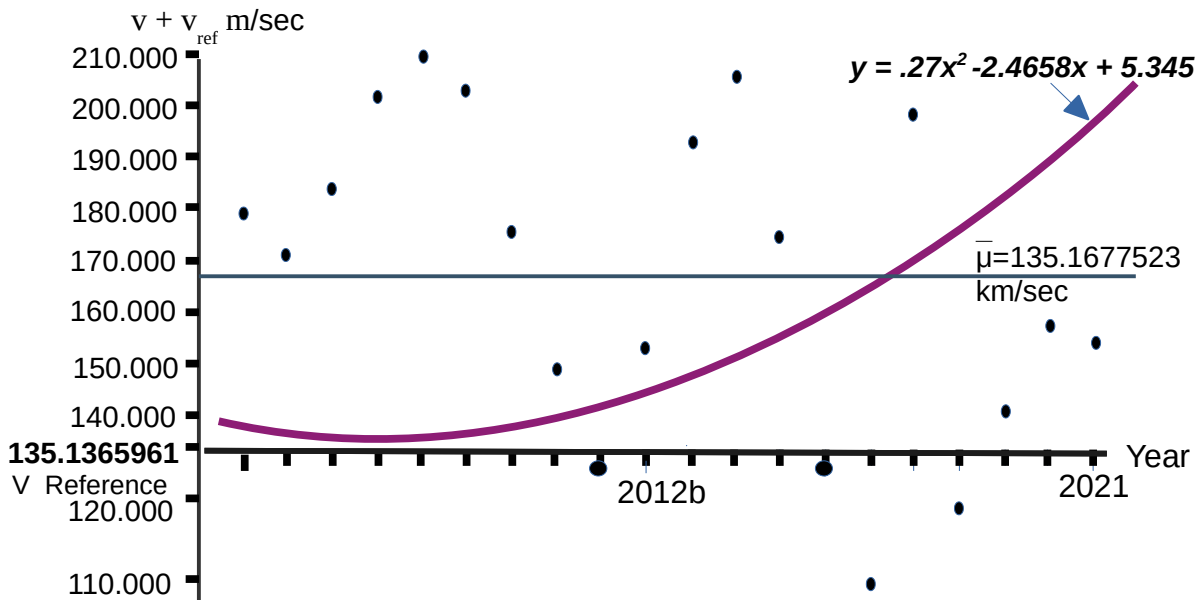


Figure 10-3: Uptrend in Distance of Perihelion over Twenty Orbits

In a like manner, we examined the velocity of BD19 throughout our sample of twenty perihelia from 2005 to 2021a (January 2021). The scatter of the data points does not lend itself to simple linear regression analysis. In the case of velocity at perihelion, therefore, we use a non-linear regression [2] to find an approximate polynomial curve to fit the data, which should meet the objective in this analysis to detect and show the increasing energy and velocity of BD19 during the twenty orbits. The result of the non-linear regression is shown in *Figure 10-4*. The general trend in the velocity data is upward since 2005. There may be an understatement of the perihelion distance by JPL in that data

base, since the reference velocity, v_{REF} , which computes from the distance r at perihelion and a the semi-major axis, is *lower* than the mean velocity of all values from twenty orbits; which may be an indicator in itself of an upward trend in the velocity of BD19 at perihelia. The upward slope in the general trend over time may also be affected slightly by less accurate older data. The polynomial fit that results will be compared against the November 2021b perihelion as a further check on the upward trend of the perihelion velocity.

The correlation of the data to the suspected acceleration effect of MOND near the Sun will converge from these different data and the analyses to show that both velocity and distance are increasing with the MOND acceleration near the Sun. There is a definite trend of higher velocities and greater distances during the twenty orbits studied in this segment of our research. The complication of various lesser influences, as modelled by the JPL “osculating elements” we believe does not override, but may “mask” the empirical evidence that is shown by these straightforward analyses of the MOND influence within the near-field of ASNF. The orbit of BD19 will thus necessarily change to reflect the added acceleration near perihelion.



Increasing velocity at perihelion for BD19 using JPL reference values r and a

$$v_{\text{perihelion}} = \sqrt{(\mu(2/r - 1/a))} = 136.1365961 \text{ km/sec} = v_{\text{ref}}$$

r = distance of perihelion

a = semi-major axis

$\mu = GM = 1.32712440018$

Figure 10-4 Non-linear regression analysis of BD19 velocity over twenty orbits [2]

Previous perihelia do appear to show the acceleration affect of MOND very near the Sun; not only is there an increased velocity, but there is also evidence for an *amplification* effect that provides added acceleration during the time of approach to perihelion. The MOND acceleration, as computed from

the Sun-Galaxy parameters in Section 1, is on the order of 10^{-11} m/sec², which is quite small. However, over the time of perihelion approach of approximately ~130 hours, this will accumulate to an acceleration 10^{-6} m/sec² in magnitude, which during the approach would result in a mean velocity change of $+\Delta\bar{v} = 6.05$ m/sec. The net increase *actually observed* and recorded has a mean value of +31.156 m/sec, indicating addition acceleration, i.e., amplification; indeed, the observed value is consistent with the existence of a MOND near-field non-gravity acceleration (NGA) with an amplification factor. We assume a normal distribution of data points over twenty orbits. Maximum velocity is achieved by the object at perihelion, with a *mean* value of $+\Delta v$ as shown in Table 10-2 of +31.156 m/sec. Over the twenty orbits, the velocity varies from the mean, with the standard deviation $\sigma = 0.02809$ over or under the mean of 135.1677525 km/sec, which is to say, ± 28.09 meters/sec, with a standard error of 6.28 m/sec. At a confidence interval of 80%, therefore, we can project an increase in the velocity over the mean value at perihelion of the current 2021b orbit of +8.04 m/sec. This is a conservative estimate based on the data from the perihelia; the scatter in the data points is caused presumably by various inner solar system perturbations and simulation elements injected into the orbit model, but these do not obscure the increases in velocity that persist through the data. A non-linear regression computation [Appendix 10-A-3] gives a prediction of velocity $\sim 135.200+$ km/sec for the November 5, 2021 perihelion. This is based on data and the analysis, showing a well defined up-trend. Actual observation data should confirm this result. The equation for change in the orbit, as given by Bate [4] is the standard astrodynamical equation for raising orbits:

$$+\Delta r_a = \frac{4a^2}{\mu} v_p \Delta v_p \quad (5)$$

where the height at aphelion r_a and the semi-major axis a of the orbit are directly affected by the velocity at perihelion. From this straightforward analysis, and observing a near-field gravity increase in velocity at perihelion, we should observe a change the semi-major axis a , or the distance at perihelion, r_p , but more likely in both. Note that NASA/JPL computes their model and uses the parameter q (distance between the asteroid and the Sun at perihelion) as 0.09205383948740019 au, or 1.37716012 Gm [JPL]. However, the “distance varies with the epoch”; the orbit model used by JPL does not currently show an increasing distance of r_p . The velocity difference mean $\Delta\bar{v}_p$ calculated based upon observations over 20 orbits is +31.156 m/sec; these numerical deviations are summarized in Table 10-2, showing the data for v_p and r_p and associated orbital elements and reference values. JPL uses various “osculating elements” to simulate effects such as general relativity and other planetoid gravity influences, and that these perturbations (other planetoids and other effects in the inner solar system) may vary during each orbit. The JPL Horizons Ephemeris has not updated their reference distance or velocity, likely due to the long time interval since observations. The fact that BD19 does *not* threaten the earth makes it a **low** priority for observations and monitoring. Funding programs are all focused on Near Earth Objects (NEO’s) that cross or otherwise threaten earth: BD 19 is not one of them. That fact notwithstanding, BD19 shows in the graphs in *Figures 10-3 and 10-4* clearly positive slope-trend of increase in the distance and velocity via regression analysis. The uptrend in both velocity and distance for the asteroid BD19 will be further *confirmed* as more perihelia are recorded, as strong evidence for MOND in the near-field of L1-to-Sun within the solar system. Also importantly, the precession of BD19 observed may eventually either take it out of the near-field cone volume due to precession, and thus it may show less acceleration; or the near-field may even “capture” BD 19 within it. These possible changes warrant further observation and research, and can provide even more conclusive evidence for MOND and ASNF gravity.

Section 1b Orbital Energy with Increasing Velocity

Direct application of the energy relation *vis viva* for orbits [9]

$$\epsilon = \frac{v^2}{2} - \frac{\mu}{r} = \frac{\mu}{2a} \quad (6)$$

Shows that the increasing velocity due to the galactic, or MOND acceleration, will cause the perihelion distance r or semi-major axis a to change accordingly, or both. Our calculation of energy ϵ of the orbit has so far calculated to a mostly steady value from 5.0610469×10^8 Joule per kilogram, calculated at perihelion; a net energy increase in the orbit is the natural consequence of the injected additional MOND-ASNF acceleration. Since the velocity increase is small relative to the orbital velocity, the effect is not be detectable in current measurements; The change in energy is $v^2/2$, or $(31.156)^2/2=485.34$, so

$$4.85 \times 10^2 \text{ J/kg} / 5.06 \times 10^8 \text{ J/kg} = 9.59 \times 10^{-7} \text{ J/kg}$$

Such effects will manifest as orbit cycles accumulate, and as they are observed with greater accuracy using radar astrometry. As of the twenty orbits studied, the change in r_p projects forward as ~ 3000 km distance per perihelion, which we propose is due to the near-field acceleration, and therefore a mean increase in velocity of $+31.156$ m/sec. Summed together as a generalized qualitative relation,

$$\epsilon + \Delta\epsilon = \frac{((v + \Delta v))^2}{2} - \frac{\mu}{r + \Delta r} = \frac{\mu}{2(a + \Delta a)} \quad (7)$$

Shows the resulting in a semi-major axis increase, and therefore the orbit will “grow” over time, due to the galactic MOND acceleration.

To summarize, this BD19 analysis strongly implies the MOND acceleration is evident in the data over a twenty orbit period, from 2005 to 2021. We have shown that both the minimum distance r_p at perihelion, as well as the velocity at perihelion, are increasing over time. This is empirical evidence for MOND acceleration in the near-field cone between the Sun and the Lagrange point L1 with the galaxy. The data reflects the MOND near-field acceleration as the direct velocity increase observed mean of $+31.156$ m/sec.

Whereas MOND is the *empirical* indication of added accelerations, we now propose ASNF as the physical mechanism or *cause* of MOND. Section 2 will establish an asymmetric near-field gravity model *ASNF* that is based upon the very large scale mass and distance ratios, i.e., Galactic Scaling Ratio’s (GSR’s), which we propose are responsible for the leverage of galaxies to control their star populations. We propose how Diffusion Gravity can actually generate or *amplify* acceleration in the near field volume between stars and their L1 point with the galaxy.

Section 2 Scaling Ratios and Dirac Large Number Hypothesis Indicate *Extreme Leverage*

We have presented evidence that MOND likely does *accelerate* a real test particle in a near-Sun orbit; now we review the Asymmetric Near-Field ASNF gravity model and how Diffusion Gravity explains MOND acceleration in the Sun’s near-field, as was presented in [15]. Ironically, the near-field model begins with the very large scales of galaxies. Consider that gravity is normally a “weak” force that is 10^{-40} the magnitude of the EM force; this important difference was studied by the physicist P.A.M. Dirac, in his 1937 *Large Number Hypothesis (LNH)* [11,12,13], wherein he noted the magnitude difference of 10^{40} between electromagnetism and gravity is seemingly an “irreconcilable” challenge in terms of likening or comparing the two phenomena, let alone the understanding, measurement and

control of gravity. The proposal herein is that in the extreme case of the L1 point being very near an orbiting star, we find an amplified gravitational potential sufficient to force and maintain the constant velocity of orbiting stars. Within the concentrated conical near-field gravity potential inside the L1 point of the orbiting star, there is then an extreme potential gradient, i.e., force. Large enough ratios, i.e., leverage, of mass and distance **boost** the gravitational force out of a “weak” field regime to a strong localized near-field. This is expressed quantitatively by the *Galactic Scaling Ratio*:

$$\mathbf{GSR} = \frac{\mathbf{Mm}}{\mathbf{R}_{Gal}r_{L1}} \quad (8)$$

where M = Galactic mass inside the Sun’s orbit, m = sun’s (solar) mass = \odot , R_{Gal} = distance to the center of the galaxy, and r_{L1} = distance from a star to L1 with its galaxy. The Galactic Scaling Ratio (GSR) for our own Sun is thus obtained $\sim 10^{70} / \sim 10^{30}$ which results in $\sim 10^{40}$, using current estimates for masses and distances. This suggests a *modified force law at galactic scale*, $\mathbf{F} = \mathbf{G}(\mathbf{GSR})$, with \mathbf{G} the *gravitational constant, that is different* from the standard Newtonian gravity equation $\mathbf{F} = \mathbf{GMm}/r^2$. We propose, moreover, that Equation (8) more accurately expresses the extreme *asymmetry of mass and distance*, where we know that the distance r_{L1} to the L1 point will always remain extremely small relative to R_{Gal} . This stronger *near-field* gravity results in each star adjusting its position relative to its L1 point [18], in accordance with the **Principle of Least Action (PoLA)**, i.e., by virtue of the reactive amplified near-field gravitational force inside the L1 point (which is itself at zero potential). Appendix 10-A-1 provides the calculations for the *PoLA effect* upon stars beyond the MOND radius.

GSR’s can be calculated from observations and estimates for mass and distance; this will enable researchers to determine the scale ratios for thousands of galaxies, and to characterize their constant velocity profiles, which in turn can provide predictive characterization. For example, the Sun in the Milky Way Galaxy (MWG) mass scaling ratio (no “dark matter”) is estimated to be on the order of $10^{10} M_{\odot}$ solar mass [NASA], while galaxies generally range from $10^8 M_{\odot}$ (for dwarf and ultra-diffuse) to $10^{14} M_{\odot}$ (for largest super-spirals). Distance scales (size) of galaxies range from dwarf size radius of $\sim 10k$ light years (10^{20} m) to $\sim 400k$ light years (4×10^{21}) [wiki]. By using Newtonian gravity potentials we find a star’s L1 Lagrange or EquiPotential (EP) balance point with its parent galaxy between the center of the galaxy and an orbiting star (e.g., see Zhao in [50]); we equate the two potentials (galactic and star) to find the point of equipotential:

$$GM/R = Gm/r$$

$$M/m = R/r_{L1} \quad \text{so,} \quad Rm/M = r_{L1} \quad (9)$$

which then gives the *distance* of the L1 as r_{L1} to the orbiting star, for example, the Sun has an estimated mass ratio with the MWG (within the Sun’s distance to the Galactic center) of $\sim M/m = 10^{10}$ and $R_{Gal} \sim 10^{20}$ meters/r, which in “order of magnitude” estimates $r_{L1} \sim 10^{10}$ meters in the direction of the galaxy center. This ratio of the distances for the L1 point of the Sun/star will create a configuration of gravity that **does not** normally occur at our more familiar solar system experience scales. That is, the extreme **proximity** of the L1 point to the star (but **not coincident** upon it) causes a concentrated, or amplified gravitational potential as referenced to the L1 point between the star and the galaxy. This is analogous to a very asymmetric, **VERY LONG** lever arm in classical mechanics. This is illustrated in *Figure 10-5*, which shows an augmented or amplified gravity model which concentrates the local gravity effect. At the massive scaling ratio between the galactic central mass and the orbiting stars, the asymmetry (leverage) of concentrated *virtual particle flows* from the star will thereby add to the gravitational attraction from the galactic core to augment the Newtonian

acceleration. [Note: This is not related to the Yukawa potential, that has been disproven previously in the Eöt-Wash experiments as a source of MOND acceleration].

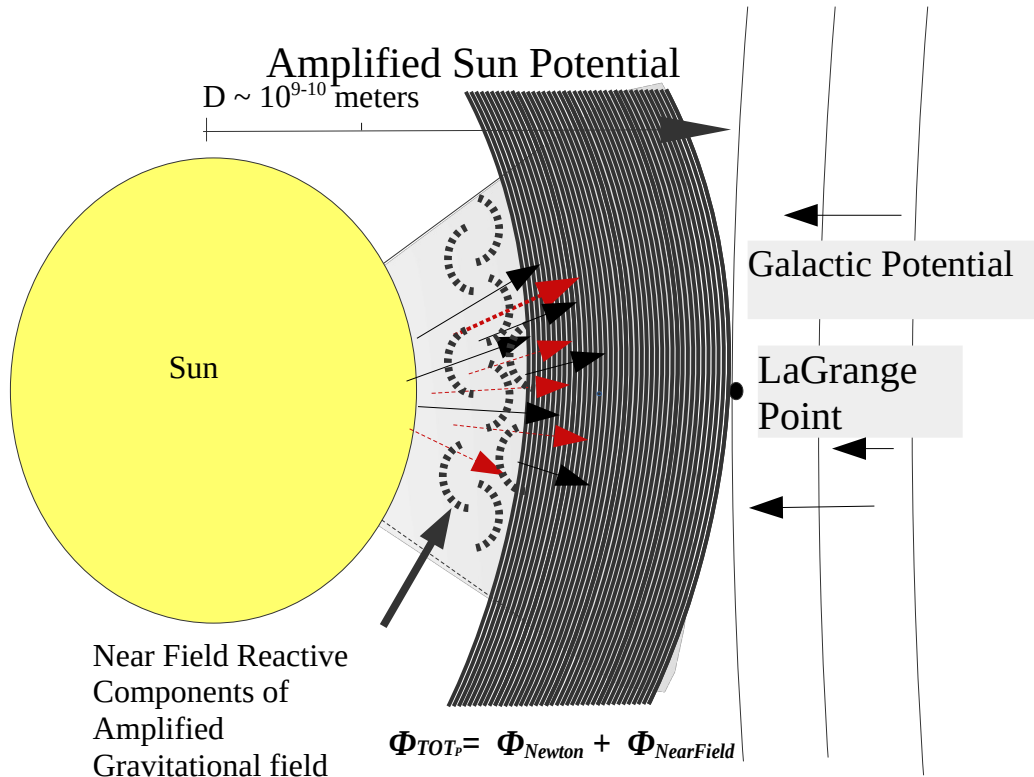


Figure 10-5 ASymmetric Near-Field Gravity Amplification and MOND

Amplification of the field (potential) gradient induces an additional gravitational force. This is normally expressed in the MOND interpolating function shown in equation (10), which reflects the conic geometric model to describe the ASNF mechanism. The *lever arm* visualization reflects the GSR, where orders of magnitude are expressed, and the ratios indicate clearly the asymmetry that powers galactic gravity, which thereby maintains stars in their constant velocity configurations.

Diffusion Gravity shows in this model how the geometry of the MOND function, F_{MOND} , corresponds to the conical geometry of virtual particle flows; previous papers [16] have given the mechanism of attraction from these virtual particle flows and annihilation; the geometric model mechanism shows how the added gravity applies to the Modified Newtonian Dynamics (MOND) as given by the “simple” interpolation function as shown in equation 10:

$$F_{MONDsimple} = \left[\frac{1}{2} + \sqrt{\frac{1}{4} + \frac{a_0}{|a_N|}} \right] \quad (10)$$

This is the MOND Function that multiplies times the Newtonian acceleration a_{NEWTON} . If we *compare* that to the equation for surface area of a cone [40]

$$S_{\text{areacone}} = \pi R^2 + \pi R^2 \sqrt{1 + \frac{h^2}{R^2}} \quad (11)$$

where the surface area of a cone is the area of the base of radius R , plus the area of the conical surface above the base, of height h , then we recognize the same form of equation. This is the DG model basis as a steradian cone. The MOND function a_{MOND} is then calculated by the geometric application of the MOND “simple” interpolating function

$$a_{\text{MOND}} = -\frac{GM}{(2R^2)} - \frac{GM}{(2R^2)} \sqrt{\left(1 + 4\frac{r^2}{R^2}\right)} \quad (12)$$

The cone’s surface represents the MOND acceleration from the interpolation function as

$$a_{\text{MOND}} = -\frac{GM}{R^2} \left[\frac{1}{2} + \frac{1}{2} \sqrt{\left(1 + 4\frac{r^2}{R^2}\right)} \right] \quad (13)$$

The surface area of the cone represents the Gaussian flux of virtual particles through the application of Gauss’ Law, where the radiated flux (to the “lens cap” of the cone) is proportional to the mass enclosed, and for a *steradian* volume:

$$\oint_{\partial V} \bar{g}(\bar{r}) \cdot d\bar{A} = -GM \quad (14)$$

The correspondence of the interpolating function to our model of near-field gravity is expressed by *steradian* geometry, and specifically the conical radiation pattern of virtual particles that emanate from star masses toward their L1. In this geometric model, the gravitational force will depend on the quantity of virtual particle flows out of the star, and that the flow will vary proportionally as the height of a cone of virtual particle flux toward the L1 point, shown as D in *Figure 10-6*. This connects interpolating functions to geometric steradial virtual particle flows from the Diffusion Gravity model to the scale ratios of galaxies. All of the virtual particles flowing through the steradian cone will concentrate at the “lens cap” for annihilation by incoming galactic virtual particle flows; the volume of the “lens cap” is $0.128 R^3$, which is the Virtual Particle volume of the *annihilation zone*, that in turn provides the strong force of attraction [16] and also a zero potential point or “fulcrum” for the Galactic Scaling Ratio (GSR) leverage, or **amplification** that galaxies exert over their star populations as the radius grows beyond the MOND radius, given by

$$r_{\text{MOND}} = \sqrt{(GM/a_0)} \quad (15)$$

The GSR operates *only beyond* the MOND radius when the Lagrange point L1 with the galaxy is a non-zero distance from the star, i.e., the distance to the L1 point from a given star vanishes for stars inside the MOND radius. Conversely, the L1 distance r_{L1} grows as the distance increases outward from the MOND radius. The amplification via this GSR is actually a concentration or amplification of potential between the star and the L1 point; this boosts the potential gradient within the radius r_{L1} , so that it also boosts the acceleration within that zone. The GSR quantifies this “leverage” in orders of magnitude (powers of ten), as a simple mathematical relation of the mass and distance in galaxies

$$\text{GSR} = M_{\text{GAL}} m_{\ast} / R_{\text{Gal}} r_{\text{L1}} \quad (16)$$

$$a_{\text{MOND}} = a_N F(a_N/a_0)$$

The interpolation function provides mathematical a description for the behaviour, but does not explain it. Note: $a_0 = 1.2 \times 10^{-10} \text{ m/sec}^2$ has been proposed as a fundamental constant. The GSR provides a *Newtonian-Like* gravity at galactic scale that *incorporates* the *asymmetric* nature of gravity at that very large scale via the Lagrange point L1 distance, which beyond the MOND radius remains very small relative to R_{Gal} . It is different from the Newtonian force law $F = GMm/r^2$, due to the *asymmetry* of size and distances. When computed for the galaxy values individually, the GSR provides an exponential magnitude that varies closely around 10^{40} as the model baseline indicator for *near-field* gravity “ideal” amplification, as has been specified in the Baryonic Tully-Fisher Relation (BTFR) [45]

$$v^4 = \sqrt{(a_0 a_N)}$$

When scaled with 1/10 proportionality constant, the GSR may provide a measure of leverage and the BTFR slope of those galaxies, i.e., mass to velocity. Examples of this suggest that the optimal 10^{40} reduces to the “sharpest” galaxy rotation curve (small dispersion) with the slope of ~ 4 as expressed in the BTFR. Recall that the Galactic Scaling Ratio embodies the *Dirac Large Number Hypothesis* ratio of 10^{40} , which translates physically into larger-scale force effect (amplification) of gravity that is operative at increasing galaxy size and scale. Therefore, $F = GMm/Rr$ should apply for all stars beyond the a_0 radius (“MOND” radius) of any given galaxy.

Correlation of the GSR to the rotation curves implies the mechanism at work in MOND and in ASNF to produce these rotation curves. The Baryonic Tully-Fisher Relation (BTFR) and similar Faber Jackson relations with the $V^\alpha \propto L$ can be modified to suggest another relation, where the exponent of velocity α is derived from the GSR as

$$v^\alpha \propto (0.1) \log_{10} \text{GSR} \quad (17)$$

such that the 10^{40} GSR ratio for gravity provides the linkage between the velocity, which is constant at r , and the baryonic mass. The significance of this linkage is contained in the GSR for each galaxy, that provides the essential “motive power” as amplified gravity from the *near-field* at each star in the galaxy; the “quality” of that ratio and its variance from 10^{40} would therefore determine the *velocity dispersion* for each galaxy.

An expression of this “quality factor” is that of the difference from a baseline value of 10^{40} , and its commensurate Baryonic Tully-Fisher slope of $4 \pm \Delta_{\text{GSR}}$, and specifically, $-\Delta_{\text{GSR}}$, which is the due to any “shortfall” of gravity (e.g., dwarf and diffuse galaxies) to maintain the constant velocity of orbiting stars. The velocity dispersion can be linked through the relation to the GSR

$$-\Delta_{\text{GSR}} \propto v_{\text{Dispersion}} \quad (18)$$

where the Δ_{GSR} translates to acceleration from GSR, and to velocity variation from a galactic mean velocity. Section 2 has presented the DG ASNF Model and its linkage to MOND; the subsequent sections will provide further plans and direction in substantiation of the model and further confirmation of MOND. The *Large Number Hypothesis* has taken shape in this model as an important driver of the mechanism for near-field gravitational effects due to *asymmetry*. The use of asymmetry is a unique feature of the ASNF model, and thereby also for MOND. Future research will investigate the role of asymmetry in galaxy cluster MOND effects, as the GSR will vary in larger scale configurations. The LNH may also drive the “sharpness” of the rotation curve and the dispersion observed in any particular galaxy, according to the relation in equations 17, 18.

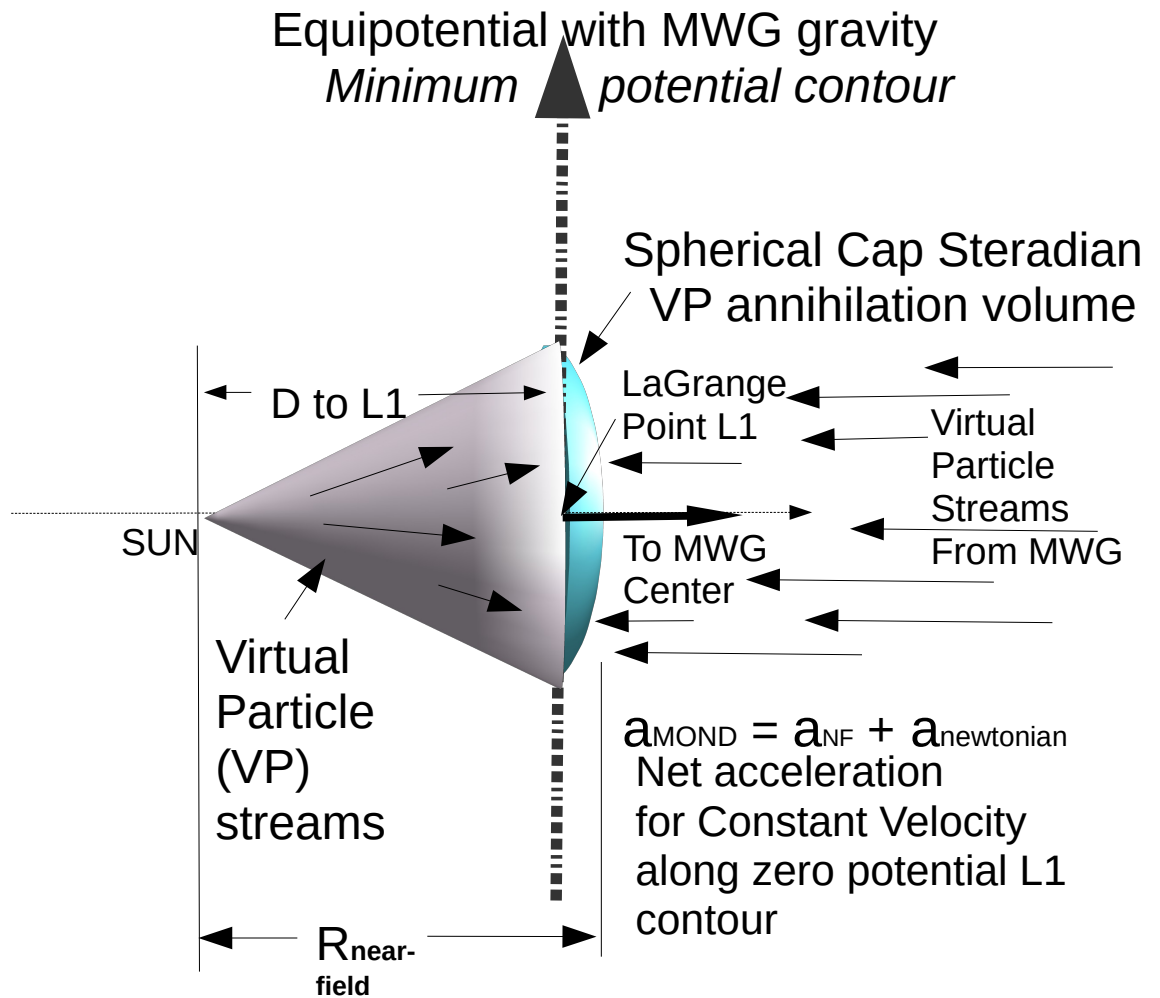


Figure 10-6 Steradian Cone Model for Diffusion Gravity

Section 3 Application of the ASNF to other Test Cases

The model and the evidence presented in this report reflects and integrates the actual observations of the asteroid near-Sun orbit; more instances of this type of dynamic interaction will provide further confirmation and refinement of the model. Specifically, the near-field gravity effect must be verified through analysis of other close passages by asteroids near the Sun, within the L1 distance of 40M km. Such data and opportunities do exist, but they are not common, since the focus has traditionally been on general relativity “confirmation” and precession of known solar system planetoids, e.g., planet Mercury and asteroid Icarus. A previous Diffusion Gravity research report has postulated the galactic gravity effects on precession of planet Mercury [17]. Now our DG model can be applied to other near-encounters of the Sun by asteroids and spacecraft that happen to align with the near-field and the L1 point with the galaxy. In future reports, we shall incorporate more cases of asteroids or spacecraft that pass through the near-field cone of ASNF near the Sun. If aligned favorably to the L1

point to the galaxy, these object may provide another opportunity to confirm near-field gravity within the MOND-ASNF cone; it should cause a change in the orbit or precession that is “anomalous”. Confirmation of MOND in the solar system from such configurations will further confirm DG-ASNF gravity. As a side note, Cavendish experiments on earth have attempted to detect and corroborate MOND for galactic gravity effects [25]. However, such measurements offer ambiguous interpretation or confirmation, and may show rather that ASNF gravity is the cause of MOND and it would only be detectable in the near-field cone of the Sun and not generally as a ubiquitous cosmic background (external field effect) acceleration in the solar system.

Additional Transits of the Near-Sun MOND-ASNF Gravity

The MOND-ASNF questions can be answered through further evidence from analyses of data for the opportunities of near-Sun perihelia, and other observations and experiments that could include spacecraft missions. For instance, the current solar probe, the Parker Solar Probe, approaches to 6.2M km of the Sun; it may provide anomalous acceleration data, even though its orbit is generally perpendicular to the L1-to-Sun alignment, and the Sun’s gravity at such close range likely will mask any other influences. Other candidate asteroids that have close approaches to the Sun will be identified and analyzed in a similar approach as those in this report.

Section 4 Summary of Evidence From Perihelia Analyses of Asteroids

The evidence for MOND near the Sun and the L1 point of the Milky Way Galaxy is clear. Beyond that evidence, Diffusion Gravity has also provided a model to suggest causality for the MOND paradigm, and the evidence to support that model. To recapitulate the main points of discovery and analysis in this work:

- 1) A sequence of asteroid 2000 BD19 perihelia over twenty orbits provides a long-term repeating record of the near-Sun encounter of an asteroid to investigate “excess” acceleration present in those approaches through the MOND-ASNF conical volume, of a similar magnitude to the “anomalous” acceleration of the U1I/2017 asteroid. Comparison has shown that acceleration of $4.9 \times 10^{-6} \text{ m/sec}^2$ is similar in magnitude to the excess acceleration and resultant velocity increase of +17 m/sec for Oumaumau. MOND acceleration magnitude in our BD19 analysis, therefore, compares closely with that previous finding. BD19 perihelia dynamics also indicate increasing distance at perihelion of ~3000km, in addition to an increasing velocity mean of +31.156 m/sec, indicating the injection of additional acceleration into the orbit of BD19. This is astrodynamically equivalent to injecting acceleration at perihelion to raise an object higher in its orbit.
- 2) Asteroid data from BD19 provides evidence and support to the Diffusion Gravity asymmetric near-field model (ASNF) as a mechanism for MOND, when the galactic gravity and alignment are considered, i.e, the L1 point to the Milky Way Galaxy is near the sun, at a distance of approximately 40M kilometers, which we propose generates a near-field steradian “cone” of acceleration that ties to the MOND equation – which we know as the “simple” interpolation function. The L1 point location is indicated by the evidence in this perihelia study.
- 3) The leverage of galaxies over their star populations is embodied in MOND and in the Diffusion Gravity model for Asymmetric Near-Field gravity. The model follows the classical mechanical analogy of a lever arm with the fulcrum at the L1 point, and the applied leverage of the galaxy exerted in the near-field cone between the Sun and its L1 point. The ASNF acceleration between L1 and the perihelion is an actual *amplification effect* as described and explained in Section 3.

4) Leverage expressed by the Galactic Scaling Ratio can form a product with G , and provide a scaled up “Newtonian-Like” force, that directly reflects the very large-scale asymmetries as a quantitative measure of ASNF gravity:

$$F = GMm/Rr$$

The *Principle of Least Action* serves as the “governor” that is highly efficient in keeping the star at constant velocity in its orbit. The GSR also provides a linkage to the Baryonic Tully Fisher Relation (BTFR) that adds the relationship of MOND to a star velocities and dispersion within the galaxy..

5) The additional Near-Field “Non-Gravitational Acceleration” (NGA) is injected during the approach of the object to perihelion, through the conical near-field gravity of MOND.

The equation that has been presented herein is the galactic scaling ratio, or GSR, as a means of quantifying the additional “leverage” of the galaxy over its stars. When the leverage achieves $\sim 10^{40}$, then near-field amplification occurs, as explained by the *Dirac Large Number Hypothesis*. In conjunction with the *Principle of Least Action*, there may actually be a surplus of acceleration needed to keep a star at constant velocity in its galactic orbit. Similarly, the leverage ratio may fall below the 10^{40} , if the galaxy mass is small or diffuse, in which cases, this can hypothetically cause the velocity dispersions as seen in observations and galactic rotation curves, i.e., where $10^{40} > \text{GSR}$ or if $\text{GSR} < 10^{40}$; further investigation is needed to confirm and refine this estimate. We also note that galaxy clusters may have different ratios and the GSR relationship could be different in such configurations, i.e., the extreme *asymmetry* we find at galactic level MOND may be reduced, i.e., *more symmetric*, thus changing the ASNF ratio and effect. Further research is required to investigate this and how the ratio might adjust in the case of galactic clusters.

Conclusion

This report has shown a definite correlation between “excess” acceleration of the 2000 BD19 asteroid and the MOND acceleration, which arises from an Asymmetric Near-Field gravity; this conclusion results from analysis of perihelia: NASA/JPL ephemeris data shows additional velocity and increasing distance at perihelion over a twenty orbit history. The data and the trend upwards indicates a source of *near-field* gravity in the conical volume of space between the Sun and its L1 point with the galaxy. MOND acceleration is thereby indicated as it coincides with the galactic gravity “zone” near the Sun. No other source of acceleration such as radiation pressure, outgassing, general relativity, or Yarkovsky effect is sufficient to explain the additional velocity and distance of perihelion for the BD19 object. The evidence shown in this report is further validation, after the previous flyby of Oumuamau (2017) initial proof and report, that excess acceleration operates in the near-field between the Sun and the L1 point with the galaxy. Similar configuration orbit examples for other asteroids or spacecraft will provide further evidence as they are analyzed to test for the same MOND acceleration of objects passing through the near-field gravity of the Sun. These will be analyzed in future research, with the overall objective of proving both MOND as an application of the Diffusion Gravity-Asymmetric Near-Field Gravity model as an alternative explanation to “dark matter”, which cannot be shown to exist. Further analysis will confirm the Galactic Scaling Ratio **leverage** model along with the *Dirac Large Number Hypothesis* applicability up to the galactic cluster level where we can explore possible enhancements to the DG model. The conclusion we continue to formulate and validate is that Newtonian gravity behaves differently at very large scales of mass and distance, i.e., galaxy scales, in

contra-indication to the assumption that massive quantities of invisible, or “dark matter” make up large proportions of those galaxies.

The work included in this report is the original work and intellectual property of the author; all references have been cited and credited; author’s sole affiliation is professional membership in IEEE.

Acknowledgements to the *Minor Planet Center, ATLAS and NASA JPL Small Body Data Base* resources.

References

1. **Acedo, Luis.** “Modified Newtonian Gravity as an Alternative to the Dark Matter Hypothesis”. *Galaxies*. MDPI. 5(4), 74. 2017.
2. **Agri-Met Software:** Non-Linear Regression Calculator, <http://agrimetsoft.com/regressions/Nonlinear#>
3. **Angus, G.W., Famaey, B., Zhao, H.,** “Can MOND take a bullet? Analytical comparisons of three versions of MOND beyond spherical symmetry in MOND”. arXiv:astro-ph/0606216v1. 2006
4. **Bate, R.R,** Mueller, D.D., White, J.E. *Fundamentals of Astrodynamics*, Dover. 1971.
5. **Binney, James** and Tremaine, Scott. *Galactic Dynamics*. Princeton University Press. 1987.
6. **Bialy, S. Loeb, A.** “Could Solar Radiation Pressure Explain Oumuamua’s Peculiar Acceleration?” *The Astrophysical Journal Letters*, 868:L1 (5pp), 2018 November 20
7. **Blanchet, Luc** & Novak, Jerome. “Testing MOND in the Solar System”, May 2011. <http://arxiv.org/abs/1105.5815v1>.
8. **Clowe, D.,** A. Gonzalez, and M. Markevitch, *Astrophys. J.* 604, 596 (Apr. 2004), arXiv:astro-ph/0312273.
9. **Danby, J.M.A.** *Fundamentals of Celestial Mechanics*, Macmillan. 1962.
10. **Di Paolo, C and Salucci, P.** “Fundamental properties of the dark and the luminous matter from Low Surface Brightness discs”. arXiv: 2005.03520v1, 2020.
11. **Dirac, P.A.M.** (1938) “A New Basis for Cosmology”. *Proceedings of the Royal Society of London A.* 165 (921):199–208.
12. **Dirac, P.A.M.** (1937). "The Cosmological Constants". *Nature*. 139 (3512).
13. **Dirac, P.A.M.** (1974). "Cosmological Models and the Large Numbers Hypothesis". *Proceedings of the Royal Society of London A.* 338 (1615): 439–446.
14. **Famaey, B and McGaugh, S.** “Modified Newtonian Dynamics (MOND): Observational Phenomenology and Relativistic Extensions” *Living Reviews in Relativity* Volume 15, Article number:10 (2012).
15. **Fulton, D.H.** “Diffusion Gravity (9) Direct Evidence for MOND and Asymmetric Near-Field Gravity in the Solar Flyby of U1I/2017” <http://vixra.org/abs/2110.0126>
DOI: [10.13140/RG.2.2.31434.29127](https://doi.org/10.13140/RG.2.2.31434.29127)
16. **Fulton, D.H.** “Diffusion Gravity (8) Asymmetric Near-Field Gravity and MOND . April, 2021. <http://vixra.org/abs/2110.0072> DOI: [10.13140/RG.2.2.17130.85443](https://doi.org/10.13140/RG.2.2.17130.85443)

- 17. Fulton, D.H.** “Diffusion Gravity (5) Perihelion Precessions as Indicators of Galactic Gravity”. February 2020. DOI: [10.13140/RG.2.2.18095.69288](https://doi.org/10.13140/RG.2.2.18095.69288)
- 18. Fulton, D.H.** “Diffusion Gravity (4): An Alternative to Dark Matter”. November 2019 DOI: [10.13140/RG.2.2.24953.42089](https://doi.org/10.13140/RG.2.2.24953.42089).
- 19. Gerber, Paul.** “The Spatial and Temporal Propagation of Gravity” Stargard, Pomerania, 1898
- 20. GraphPad Software** Linear Regression Calculator, <http://www.graphpad.com/quickcalcs/linear1/>
- 21. Hofmeister, Anne & Criss, E.** “Constraints on Newtonian Interplanetary Point-Mass Interactions in Multicomponent Systems from the Symmetry of Their Cycles”
- 22. Jefimenko, Oleg.** *Causality Electromagnetic Induction and Gravitation.* Electret 2000.
- 23. JPL/NASA SBDB** Horizons Ephemeris. http://ssd.jpl.nasa.gov/tools/sbdb_lookup.html#/
- 24. Katz, J.I.** “Evidence against non-gravitational acceleration of 1I/2017 U1 ‘Oumuamua”, arXiv:1904.02218v1 (astro-ph). March, 2019.
- 25. Klein, Norbert.** “Evidence for Modified Newtonian Dynamics from Cavendish-type gravitational constant experiments”. *Classical and Quantum Gravity*, Vol.37, No.6. 18 Feb 2020 IOP.
- 26. Kroupa, P, Banik, I.** “Solar System limits on gravitational dipoles” arXiv:2006.06000v1 [astro-ph.EP] 10 Jun 2020.
- 27. Li, Qing, et.al.** “Measurements of the Gravitational Constant using Two Independent Methods” *Nature*, volume 560, pages 582–588. 2018.
- 28. Margot, J.L. & Georgini, J.D.** “Probing general relativity with radar astrometry in the inner solar system” *Relativity in Fundamental Astronomy Proceedings IAU Symposium No. 261*, 2009 S. A. Klioner, P. K. Seidelman & M. H. Soffel, eds.
- 29. McGaugh, Stacy S;** Schombert, James; Lelli, Frederico. “The Radial Acceleration Relation in Rotationally Supported Galaxies” arXiv:1609.05917v1 astro-ph. 2016.
- 30. McGaugh, S. S.;** Schombert, J. M.; Bothun, G. D.; de Blok, W. J. G (2000). "The Baryonic Tully-Fisher Relation". *The Astrophysical Journal Letters*. **533** (2): L99.
- 31. McGaugh, Stacy.** “Milky Way Mass Models and MOND”. *The Astrophysical Journal*, 683:137Y148, 2008 August 10.
- 32. Meech, K.J.;** Weryk, R.; Micheli, M.; Kleyna, J.T.; Hainaut, O.R.; Jedicke, R.; Wainscoat, R.J.; Chambers, K.C.;Keane, J.V.; Petric, A.; et al. “A Brief Visit From a Red and Extremely Elongated Interstellar Asteroid”. *Nature* 2017, 552, 378–381.

- 33. Micheli, M.**, Farnocchia, D., Meech, K.J., Buie, M.W., Hainaut, O.R., Prialnik, D, et. al. “Non Gravitational Acceleration in the Trajectory of 1I/2017 U1 Oumuamau”. *Nature* May 2018.
- 34. Milgrom, M.** "A modification of the Newtonian dynamics as a possible alternative to the hidden mass hypothesis". *Astrophysical Journal*. **270**: 365–370. 1983.
- 35. Milgrom, M.** MOND Effects in the Inner Solar System, 2009. <http://arxiv.org/abs/0906.4817v2>
- 35. Milgrom, M.**, “MOND fiducial specific angular momentum of disc galaxies”, arXiv:2107.03691v1 [astro-ph.GA] 8 Jul 2021.
- 36. NASA/JPL Horizons Database, 2000 BD19:** <http://ssd.jpl.nasa.gov/horizons/app.html#/>
- 37. Oumuamua**, Wikipedia, <http://en.wikipedia.org/wiki/%CA%BBOumuamua>
- 38. Rafikov, R.R.** “Spin Evolution and Cometary Interpretation of the Interstellar Minor Object 1I/2017 ‘Oumuamua”. *The Astrophysical Journal Letters*, Volume 867, Issue 1, article id. L17, pp. (2018).
- 39. Ray, Saibal.** Large Numbers Hypothesis: A Review. ResearchGate, February, 2019.
- 40. Rosser, Kathleen A.** “Modified Newtonian Gravity as the Surface Area of a Cone”. December, 2020. <https://quemadojournal.org/modified-newtonian-gravity-as-the-surface-area-of-a-cone/>
- 41. Sanders, R.H.** *Mon. Not. R. Astron. Soc.* 342, 901 (Jul. 2003), Clusters of Galaxies with Modified Newtonian Dynamics arXiv:astro-ph/0212293.
- 42. Seligman, D., Laughlin, G., Batygin, K.** “On the Anomalous Acceleration of 1I/2017 U1 ‘Oumuamua” *The Astrophysical Journal Letters*, 876:L26 (5pp), 2019 May 10
- 43. Syusina, O.M., Galushina, T.** “Determination of Yarkovsky Effect Parameter for Asteroids with Small Perihelion Distances”. *Russian Physics Journal*, November 2021.
- 44. Trilling, D.E.** “Spitzer Observations of Interstellar Object 1I/‘Oumuamua” *The Astronomical Journal*, Volume 156, Issue 6, article id. 261, pp. (2018).
- 45. Tully, R. B.; Fisher, J. R.** (1977). "A New Method of Determining Distances to Galaxies". *Astronomy and Astrophysics*. **54** (3): 661–673
- 46. VanDokkum, P.** et.al., “A Second Galaxy Missing Dark Matter In The NGC 1052 Group.” arXiv:1901.05973v3 [astro-ph.GA] 15 Mar 2019.
- 47. Wagner, T.A., Gundlach, J.H., et al.** “Torsion-balance tests of the weak equivalence principle” *IOP Classical and Quantum Gravity*. 15 August 2012 , Volume 29 Number 18.
- 49. Wilhelm, Klaus, and Dwvidi, Bhola.** “Anomalous Sun Flyby of 1I/2017 U1 (‘Oumuamua)” *Galaxies MDPI*. 2020.

48. **Galaxy Size ranges** , Wikipedia, <http://en.wikipedia.org/wiki/Galaxy>
49. **Yarkovsky Effect**, Wikipedia, 2021.
50. **Zhao, Honsheng**; Famaey, B. “Refining MOND interpolating function and TeVeS Lagrangian” arXiv:astro-ph/0512425v3 5 Jan 2006.
51. **ATLAS Warning System**: <http://www.ifa.hawaii.edu/info/press-releases/ATLAS/>
52. **Minor Planet Center**: <http://minorplanetcenter.net/iau/mpc.html>

Appendix 10-A-1 Calculations for Energy in Principle of Least Action
Asymmetric Near-Field Gravity
Addendum to Diffusion Gravity Project 11/2019
DHFulton@ieee.org

Section 1 The PoLA ratio and the Calculation of Sun “Deficit” Acceleration

The recent (11/2019) paper submitted for Diffusion Gravity has presented the conceptual framework and concepts for the Alternative to Dark Matter, including the Principle of Least Action and the gravitational Equipotential Surfaces that are the key to the assertion that Nature practices least expenditure of energy in the stellar orbits of galaxies. The calculations shown here are meant to compare *the energy required to keep a star in close proximity to the zero-potential trajectory (orbit) vice the energy of the orbiting star and its solar system mass.* We designate this the PoLA (Principle of Least Action) ratio:

$$\text{PoLA} = \frac{\text{EP-energy of star}}{\text{Kinetic-energy of star}} = \frac{m a_{EP} r_{EP}}{\frac{1}{2} m v^2}$$

where

m is the mass of the star plus its solar system, as (wikipedia) 1.0014 solar mass = 2.0028 x 10³⁰ kg.

a_{EP} is the acceleration needed to keep the star near the zero-potential contour = to be calculated here.

r_{EP} is the radius distance from the star needed to keep it “on track” for the Least Action = .75x10⁹ meters

v is the constant velocity of the star = 230 km/sec for the Sun and solar system

We are calculating the “deficit” acceleration as portrayed in the “Diffusion Gravity: An Alternative to Dark Matter” research paper. This is the difference between the apparent acceleration obtained from classical Newtonian mechanics:

$$ma = GMm/r^2$$

$$a_{\text{NEWT}} = GM/r^2$$

Now, comparing the two different calculations, assuming

G = Universal Gravitational Constant = 6.67 x 10⁻¹¹ m³/kg m²

M = Mass Milky Way inside Sun radius = 9 x 10¹⁰ solar mass x 2.0028 10³⁰ kg = 18.03 x 10⁴⁰

kg (this is an estimate, since there is continuing uncertainty in the mass of Milky Way Galaxy)

luminous matter in the Milky Way Galaxy, taken as 9x10¹⁰ solar masses, inside the Sun’s

radius.

m = Mass of the Sun/Solar System = 2.0028 x 10³⁰ kg

r = Distance from Milky Way Center of Sun = 2.6 x 10²⁰ m

v = Velocity of the Sun (average) in orbit of Milky Way Galaxy = 230 x10³ m/sec

The Newtonian acceleration the Sun

$$= \sqrt{(6.67 \times 10^{-11})(9 \times 10^{10} \text{ solar mass})(2.001 \times 10^{30} \text{ kg/solar-mass})/(2.6 \times 10^{20} \text{ m})^2}$$

$$GM/r^2 = (12.09 \times 10^{30}/6.76 \times 10^{40})$$

$$a_{\text{NEWT}} = 1.78 \times 10^{-10} \text{ m/sec}^2$$

And the $ma = mv^2/r$ Kepler law gives observed centripetal accel $a_r = v^2/r = (230 \times 10^3 \text{ m/sec})^2 / 2.6 \times 10^{20} \text{ m}$

$$a_r = 5.29 \times 10^{10} / 2.6 \times 10^{20} \text{ m/sec}^2$$

$$a_r = 2.03 \times 10^{-10} \text{ m/sec}^2$$

This gives the shortfall or deficit of acceleration from visible matter to the Keplerian observed centripetal acceleration to be

$$a_{\text{deficit}} = a_r - a_{\text{NEWT}} = 2.03 \times 10^{-10} - 1.78 \times 10^{-10} \text{ m/sec}^2$$

$$a_{\text{deficit}} = 0.25 \text{ m/sec}^2$$

Comparing the two values gives an estimate based on widely available and accepted measured physical values and constants.

The above calculations are only meant to show (qualitatively) that there is a deficit, or shortfall of the acceleration from the estimates of visible matter provided by various sources (the “official” estimates contribute to have uncertainty). The number is likely conservative, and there are higher estimates now available for the mass of the Milky Way Galaxy, but these have not been verified to the extent of the $9 \times 10^9 \text{ sm}$ used here, and many contain “dark matter” estimates. The perceived shortfall of acceleration can be modelled and explained with possible alternatives to “dark matter”. The primary method for the Diffusion Gravity model is to apply the the Principle of Least Action and the Equipotential surface proximate to the Sun’s orbit to determine the amount of energy that is required to compensate for the shortfall. In the case of the Sun, we showed that the centripetal a_r “needed” to equal the Keplerian “required” by v^2/r (that is observed) may be in the $0.25 \times 10^{-10} \text{ m/sec}^2$ range.

Section 2 Applying Diffusion Gravity Principle of Least Action (PoLA) model to acceleration deficit using Energy Considerations

This section applies the DG Model with its PoLA assumption, wherein a mechanism shown in the research paper “Diffusion Gravity (4): An Alternative to Dark Matter” is used as an explanation for the perceived deficit of Newtonian acceleration as calculated in the previous section 1.

So we can now calculate the amount of energy per $.1 \times 10^{-10} \text{ m/sec}^2$ so we can use a linear model for the amount of energy to keep the Sun near the equipotential surface.

$$\text{Force} \times \text{Distance} = \text{Work} = \text{Energy}$$

$$\text{mass} \times \text{acceleration} \times \text{distance} = \text{energy needed}$$

to keep the Sun near the equipotential surface. Mass of the sun is $2.004 \times 10^{30} \text{ kg}$; distance assumed [4] is the half diameter of the Sun = $.75 \times 10^9 \text{ m}$. So for each $.1 \times 10^{-10}$ increment of acceleration, the energy needed would be

$$(2.004 \times 10^{30} \text{ kg})(.1 \times 10^{-10} \text{ m/sec}^2)(.75 \times 10^9 \text{ m}) = .150 \times 10^{29} \text{ joule}$$

If we compare that to the energy of the Sun moving in its orbit

$$\frac{1}{2} mv^2 = (1.002 \times 10^{30} \text{ kg})(230 \text{ km/sec})^2 = 5.30 \times 10^{40} \text{ joule}$$

So the ratio or fraction of the energy needed to keep the sun in a least-action proximity to the equipotential surface per 0.1×10^{-10} acceleration (to compensate for the shortfall due to “missing” matter) is

$$\frac{.150 \times 10^{29}}{5.30 \times 10^{40}} = .0283 \times 10^{-11} = 2.83 \times 10^{-13} \sim \text{3 parts in ten trillion}$$

The importance is that it is a tiny amount required per “nudge” to keep the Sun (or any star) in its minimal energy path. The constant velocity therefore can easily be maintained by this mechanism of “least action” that requires minimal energy. The Diffusion Gravity gradient provides the driving force to implement this “minimizer” energy function near the equipotential surface, as was portrayed in Section 2 in the work cited[4]. Even if a star required a “nudge” of $.25 \times 10^{-10}$ as we calculated in section 1 above, that would make a minute difference in the amount of energy needed as a percentage of the kinetic energy of the star. For the Sun in these calculations, $.25/.1 = 2.5 \times 2.83 \times 10^{-13}$ will still amount only to about 9 parts in ten trillion. We conclude that the PoLA is very much likely in operation and an essential part of the dynamics of galactic rotation curves.

The increases in some velocity profiles suggest that the process of energy transfer from the kinetic to the transverse (centripetal) a_r and the reverse process also, where the Milky Way Galaxy may impart additional acceleration a to increase the velocity of the stars. The PoLA mechanism shown, therefore, may be symmetric, so that changes in a_r could change v , which suggests that the process may not be strictly entropic, but reversible. The galactic rotation profiles can be indicators then, of an energy exchange process that is operating to flatten or even increase the velocities of the stars in their orbits. This may be in the form of harmonic variations in a_r , or some similar mechanism that ensures a constant star velocity with a gravitational mechanism.

These model concepts for the Diffusion Gravity model show that there is a very viable alternative to “dark matter” through the Milky Way Galaxy dynamics, which does not depend on a halo of “dark matter”.

Section 3 Conclusion

Nature practices extreme conservation and efficiency even at galactic scale. The PoLA and Equipotential surface concepts and component model extensions of the Diffusion Gravity Model will be incorporated and integrated into the DG Theory in subsequent additional research papers.

Reference:

Diffusion Gravity (4): An Alternative to Dark Matter, 11/2019

www.researchgate.net/publication/337261681_Diffusion_Gravity_4_An_Alternative_to_Dark_Matter

Appendix 10-A-2 Analyses of Data Linear Regression

Fit of data as Up-Trend Slope.

Year x	Distance y		xy	x2
1	1.376284765		1.376284765	1
2	1.376435821		2.752871642	4
3	1.376166441		4.128499323	9
4	1.375813096		5.503252384	16
5	1.375722849		6.878614245	25
6	1.375857518		8.255145108	36
7	1.376361093		9.634527651	49
8	1.376883767		11.015070140	64
9	1.377134572		12.394211150	81
10	1.376762220		13.767622200	100
11	1.376054962		15.136604580	121
12	1.375763432		16.509161180	144
13	1.376345407		17.892490290	169
14	1.377158739		19.280222350	196
15	1.377600923		20.664013850	225
16	1.377224973		22.035599570	256
17	1.377326459		23.414549800	289
18	1.377010793		24.786194270	324
19	1.376681646		26.156951270	361
20	1.376446956		27.528939120	400
205	27.53103643		284.98232560	2870

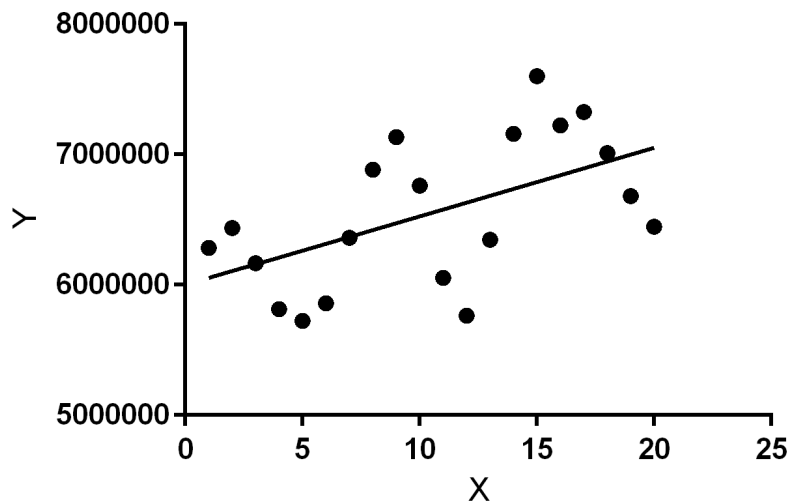


Figure 10-A-2 Linear Regression Direct Output Graphic GraphPad

Appendix 10-A-3
 From AgriMet Software:

Paste Y here. Each sample in one line. (independent)	Paste X here. Each sample in one line. (dependent)
42.54	1
34.73	2
48.67	3
66.99	4
71.86	5
64.69	6
38.58	7
11.50	8
-1.49	9
17.80	10
54.45	11
69.57	12
39.40	13
-2.74	14
-25.63	15
57.48	16
-11.43	17
4.92	18
21.97	19
19.29	20

Function = $f(x) = Y = 0.27 * X^2 + -2.4658 * X + 5.345$
F-Value is: 0.39
Significant Level is: 0.05
Significant is: False
P-Value: 0.97850988
R2 = -1.3534
Root Mean Squared Errors: 43.4986

<http://agrimetsoft.com/regressions/Nonlinear#>